

1
2 **Influence of pulsed electric fields and mitochondria-cytoskeleton interactions on cell**
3 **respiration**

4
5
6 I Goswami, JB Perry, MA Allen, DA Brown, MR von Spakovsky, SS Verbridge
7
8
9
10
11
12
13
14
15
16
17
18
19
20
21
22
23
24
25
26
27
28
29
30
31
32
33

1 **ABSTRACT**

2 Pulsed electric fields with microsecond pulse width (μ sPEF) are used clinically, namely,
3 IRE/Nanoknife for soft tissue tumor ablation. The μ sPEF pulse parameters used in IRE (0.5-1
4 kV/cm, 80-100 pulses, \sim 100 μ s each, 1 Hz frequency) may cause an internal field to develop within
5 the cell due to disruption of the outer cell membrane and subsequent penetration of the electric
6 field. An internal field may disrupt voltage sensitive mitochondria, although the research literature
7 has been relatively unclear regarding whether or not such disruptions occur with μ sPEFs. The
8 present investigation reports the influence of clinically used μ sPEF parameters on mitochondrial
9 respiration in live cells. Using a high throughput Agilent Seahorse machine, it was observed that
10 μ sPEF exposure comprising of 80 pulses with amplitudes 600 or 700 V/cm did not alter
11 mitochondrial respiration in 4T1 cells measured after an overnight post-exposure recovery. To
12 record alterations in mitochondrial function immediately after μ sPEF exposure, high resolution
13 respirometry was used to measure electron transport chain state via responses to glutamate-malate
14 and ADP, and mitochondrial membrane potential via response to FCCP. In addition to measuring
15 immediate mitochondrial responses to μ sPEF exposure, measurements were also made on cells
16 permeabilized using digitonin, and those with compromised cytoskeleton due to actin
17 depolymerization via treatment with the drug Latrunculin B. The former treatment was used as a
18 control to tease out the effects of plasma membrane permeabilization, while the latter was used to
19 investigate indirect effects on the mitochondria that may occur if μ sPEFs impact the cytoskeleton
20 on which the mitochondria are anchored. Based on the results it was concluded that, within the
21 pulse parameters tested, μ sPEFs alone do not hinder mitochondrial physiology, but can be used to
22 impact the mitochondria upon compromising the actin. Mitochondrial susceptibility to μ sPEF after
23 actin depolymerization provides a novel avenue for cancer therapeutics.

24

25

26

27

28

29

30

31

32

33

34

35

36

37

38

39

40

1 1 INTRODUCTION

2 The mitochondrial network generates metabolites critical for the biosynthetic and catabolic
3 processes inside the cell. Substrates from food are broken down and ultimately channeled to the
4 electron transport chain (ETC), in which a series of reduction/oxidation reactions along the inner
5 mitochondrial membrane are coupled to proton pumping. The resulting proton gradient creates and
6 sustains mitochondrial membrane potential critical for bioenergetic homeostasis. In mammalian
7 cells, molecular oxygen is the terminal electron acceptor in the ETC. Accordingly, measurement
8 of mitochondrial oxygen consumption provides a reliable measurement of bioenergetic status.
9 Beyond its bioenergetic and biosynthetic functionalities, the mitochondrion is now understood to
10 also act as a signaling organelle. For example, an ETC protein cytochrome C is released by the
11 mitochondrion to initiate cell death. Furthermore, the mitochondrion contains its own DNA and
12 the signaling between the mitochondrion and the nucleus is now thought to regulate many cellular
13 processes including those involved in cancer progression. The interested reader is directed to the
14 review in Chandel (2014). Due to the role of the mitochondrion in cellular processes, particularly
15 in cell death, there is an increasing interest in understanding how applied exogenous transient
16 pulsed electric fields (PEFs) that are used in clinical tumor ablation interact with the mitochondrial
17 network.

18 A representative clinically used PEF pulse train consists 80 to 100 square wave pulses each of
19 width 100 μ s delivered via electrodes into the tissue at a frequency of 1 Hz. Note that the clinical
20 modality using PEFs is known as irreversible electroporation (IRE) or Nanoknife (Jourabchi et al.,
21 2014; Martin et al., 2017; Scheffer et al., 2015, 2016; Scheltema et al., 2016; Trimmer et al., 2015).
22 The delivery of energy via PEFs disrupts the plasma membrane, causing loss of cell homeostasis,
23 which can lead to cell death if the cell does not recover from the perturbation. To target organelles
24 such as the mitochondrion, investigators have suggested leveraging the electrical property of the
25 outer cell bilayer membrane. The permittivity of biological lipid cell membranes decreases as the
26 frequency of an exogenous time-oscillating electric field is increased. Similarly, the conductivity
27 of these membranes increases with an increase in frequency of the exogenous oscillating electric
28 field. Thus, when a cell is exposed to an exogenous square wave electric field, the harmonics (or
29 frequency components) dictate the electrical property of the membrane. It has been theoretically
30 and experimentally argued (e.g., Schoenbach *et al.* (1997) and Ivey *et al.*, (2015)) that reducing
31 the pulse width of the square wave electric field to the order of a sub-microsecond or nanosecond,
32 and thereby increasing the number of high frequency harmonic components, can make the outer
33 lipid membrane conductive to the electric field and allow most of the exogenous field to reach the
34 cytoplasmic compartment. An excellent summary of investigations using exogenous fields with
35 nanosecond pulse widths is given in Napotnik *et al.* (2016). As indicated in the research literature,
36 such an approach of increasing higher frequency components of an exogenous square wave electric
37 field has been proposed as a way of targeting the mitochondria with limited impact on the outer
38 cell lipid membrane.

39 However, contradictory findings have been reported in terms of the impact of nanosecond PEF
40 (nsPEF) on cytochrome C release by mitochondria with some findings indicating no release and
41 others release. Clearly, it would be of benefit in cancer therapeutics for the latter and not the former
42 to be true. For example, an investigation from 2003 (Beebe *et al.*, 2003) reported exposure of
43 human Jurkat and HL-60 cells to a nsPEF train with varying pulse widths (10-300 ns per pulse)
44 and field strengths (36-150 kV/cm). Note that across all their treatment conditions, an energy
45 density of 1.7 J/cc was delivered. Immediately after exposure, cell fractionation was performed to
46 obtain cytosolic proteins. Immunoblot measurement of cytochrome C revealed an increase in the

1 protein levels with increasing pulse width. The increased level of cytochrome C in the cytosolic
2 compartment was associated directly with the impact of the nsPEF on the mitochondria. A more
3 recent study (Estlack *et al.*, 2014b) exposed human T-lymphocytes Jurkat cells and monocytes
4 U937 cells to a pulse train of a 100 pulses each with a 10 ns width and 1 Hz frequency. Two field
5 strengths were used: 50 kV/cm and 150 kV/cm. The expressions of caspase 9 and BAX involved
6 in mitochondria mediated cell death was not detected in either cell line upon exposure to the
7 nsPEF. Immunoblot measurements also confirmed no release of cytochrome C in either case.

8 Contradictory findings have also been made with regard to the impact of nsPEF on
9 mitochondrial membrane potential, which could indicate whether or not the exogenous field
10 permeabilizes the mitochondrial membrane and, thus, influences the proton gradient across it
11 critical for ATP production. For example in Napotnik *et al.* (2012), mitochondrial membrane
12 potential fluorescent dyes rhodamine R123 and tetramethyl rhodamine ethyl ester (TMRE) were
13 used to stain lymphocyte Jurkat cells prior to nsPEF delivery. After the staining and washing steps,
14 cells were exposed to 5 or more pulses each with widths of 4 ns delivered at a frequency of 1 kHz
15 with a field magnitude of 100 kV/cm. Fluorescent signals were captured using a microscope, and
16 raw units were compared before and after exposure to the nsPEF. The investigators reported a
17 reduction by 76% and 78% in the raw units of R123 and TMRE, respectively, upon nsPEF
18 exposure. Moreover, there was an induced change of 61% and 12% in the raw units of R123 and
19 TMRE, respectively, in cells treated with protonophore carbonyl cyanide-p-
20 trifluoromethoxyphenylhydrazone (FCCP) as a positive control, which disrupts the mitochondrial
21 membrane potential. Another study using human liver cancer SMMC-7221 cells compared
22 mitochondrial membrane potentials resulting from different microsecond and nanosecond pulse
23 treatments (Mi *et al.*, 2009). Similar to the previously mentioned study, cells were stained with the
24 R123 dye and washed before exposure to the PEF. The pulse train for the microsecond PEF
25 consisted of an exposure of 8.5 minutes to 200 V/cm fields and pulse widths of 1.3 μ s delivered at
26 a frequency of 50 Hz. The nanosecond pulses had a similar frequency and exposure time with a
27 higher field magnitude (600 V/cm) and a pulse width of 100 ns. Note that this study used an
28 exponentially decaying pulse as opposed to the square pulses used in the other mentioned
29 investigation. As in the previous study, they also report a lowering of the raw fluorescent units in
30 cells treated with either pulse train, although the reduction was steeper in the nanosecond pulse
31 treated cells. This was indicative of the mitochondrial membrane potential being perturbed by both
32 the microsecond and nanosecond pulses.

33 While the two studies described in the previous paragraph on intact cells provide evidence of
34 the PEF (or more specifically the nsPEF) impacting the mitochondrial membrane potential, they
35 seem to contradict findings on isolated mitochondria by Estlack *et al.* (2014a). In this study, Jurkat
36 and U937 cells were used to isolate mitochondria, which were then exposed to 50 kV/cm and 10-
37 100 pulses each with a 10 ns width delivered at a frequency of 1 Hz. The oxygen consumption was
38 measured using an Agilent Seahorse machine an hour after exposure. The study reported no
39 alterations in mitochondrial respiration with nsPEF exposure, indicative of no effect of the nsPEF
40 train used on mitochondrial membrane potential. This contradiction between findings on intact
41 cells and isolated mitochondria leads to the question of whether or not the differences are due to
42 the complex interactions, both structurally and functionally, that the mitochondria inside the intact
43 cells have with other cell structures such as the cell cytoskeleton on which each mitochondrion is
44 anchored. A possibility, thus, exists that the impact of the nsPEF on the mitochondria is an indirect
45 effect via alterations in some other cellular component. As mentioned earlier, it is hypothesized
46 that the higher frequency harmonics of nsPEFs have limited impact on the outer cell membrane.

1 It, however, cannot be completely ruled out that nsPEFs do indeed change the intracellular ionic
2 concentrations brought about by cell membrane permeabilization. Such alterations in intracellular
3 environment could also effect mitochondrial respirations.

4 In contrast, it has been argued that microsecond pulse parameters used in clinical settings do
5 impact mitochondrial membrane potential due to outer cell membrane permeabilization. For
6 example, theoretical predictions by Esser *et al.* (2010) suggest that upon membrane
7 permeabilization, voltage sensitive organelles such as the mitochondria are exposed to the
8 exogenous PEF. However, the question arises as to what μ sPEF amplitudes impact the
9 mitochondrial membrane potential or physiology? A study by Reynaud *et al.* (1989) on isolated
10 rat liver mitochondria suggests that the PEF pulse amplitude for microsecond pulse trains would
11 have to be extremely high to alter mitochondrial physiology. Briefly, isolated rat liver
12 mitochondria were exposed to 5 PEF pulses each with a 100 μ s pulse width and a frequency of 0.2
13 Hz. Increased mitochondrial respiration was indirectly indicated by an increased basal oxygen
14 consumption rate for field strengths up to 2 kV/cm, measured immediately after exposure using
15 Clark-type electrodes. Mitochondrial damage indicated by fusion of the mitochondria was only
16 seen beyond 1 kV/cm. However exposure of live cell mitochondria to such high fields may not be
17 practical, as we have previously shown in Goswami *et al.* (2017), a field strength above 700 V/cm
18 with clinically used pulse parameters (width: 100 μ s; frequency: 1 Hz; pulses: 80-100) results in
19 very limited cell viability.

20 Nevertheless, these studies highlight that the influence of nanosecond and microsecond PEFs
21 on mitochondria is still not completely understood. Specifically, a mechanistic understanding
22 needs to be developed on how these PEFs, specifically those used in a clinical setting, impact cell
23 structure and cell signaling. To address this gap in our understanding, the following sections
24 present the results of an investigation of mitochondrial responses in murine triple negative breast
25 cancer 4T1 cells exposed to μ sPEFs using clinical parameters previously shown to influence cell
26 signaling (Goswami *et al.*, 2017). The goal is to determine whether or not mitochondrial
27 perturbations recorded after μ sPEF exposure are unique to an electric field effect or whether
28 similar perturbations can be brought about by non-electrical means. Respecting the structural and
29 functional complexity that exists in a cell, an investigation is also made of whether or not a
30 disruption of the actin cytoskeleton triggers a higher susceptibility of the mitochondria to μ sPEF
31 perturbation.

32 **2 MATERIALS & METHODS**

33 **2.1 Cell line and culture conditions:** The triple negative breast cancer murine cell line 4T1 was
34 purchased from American Type Culture Collection (ATCC, Catalog number: CRL-2539). The 4T1
35 cells were maintained in an RPMI-1640 culture medium supplemented with 10% (by volume) fetal
36 bovine serum (FBS) and 1% (by volume) penicillin streptomycin (PS). Cells were sustained in
37 humidified incubators at 37 °C and 5% CO₂ and were sub-cultured at approximately 80%
38 confluence, while 0.25% Trypsin-EDTA solution was used for detachment. All experiments were
39 performed within the first ten sub-cultures.

1 **2.2 Pulsed electric field exposure protocol:** The protocol was previously reported by Goswami
2 *et al.* (2017). Briefly, following the harvest, the cell pellet was washed with phosphate buffered
3 saline without calcium and magnesium (PBS^{-/-}; Santa Cruz Biotechnology) and re-suspended in a
4 basal growth media with neither serum nor PS. Approximately 6-8 million cells/cuvette were
5 transferred to 4 mm electroporation cuvettes (Mirus Bio LLC) in a volume of 600 mL. Each cuvette
6 was placed in a holder through which the cells were exposed to electric field. The electric voltage
7 required for the μ sPEF exposure was generated using an electroporation unit (Harvard Apparatus,
8 USA). Short pulses of 100 μ s were delivered at a frequency of 1 Hertz. The number of pulses was
9 kept constant at 80. The electric field strength reported in this article was calculated by taking the
10 ratio of electric voltage applied to the distance between the electrodes in the cuvette (4 mm). Two
11 different field strengths were investigated: 600 V/cm and 700 V/cm. The viabilities of the 4T1
12 cells exposed to these field strengths were reported by our earlier study to be 80% (600 V/cm) and
13 40% (700 V/cm) when evaluated after overnight incubation post-treatment (Goswami *et al.*, 2017).
14 For the untreated controls, cells were transferred to cuvettes and kept in the cuvette for the same
15 duration as the treatment groups without application of an electric field.

16 **2.3 Mitochondrial respiration measurements in an Agilent Seahorse XF machine:** After
17 exposure to the PEFs, cells (including the untreated controls) were allowed to recover for
18 approximately thirty minutes in ice while total cell count was made using a hemocytometer for
19 each sample. Approximately 40,000 cells were seeded in each well of an Agilent Seahorse (Santa
20 Clara, California, USA) XF24 tissue culture plate and allowed to incubate overnight in a cell
21 culture incubator at 37 °C and 5% CO₂. After overnight incubation, samples were washed with
22 assay buffer (Seahorse XF Base Medium, 10mM pyruvate, 10mM glucose, and 2mM glutamax)
23 after which mitochondrial respiration via oxygen consumption rate (OCR) was measured in the
24 XF24 plate reader following our established protocol (Dai *et al.*, 2016). Injections of 2 μ M ATPase
25 inhibitor Oligomycin, 0.5 μ M protonophore carbonyl cyanide-p-
26 trifluoromethoxyphenylhydrazone (FCCP), and 1 μ M electron transport chain complex III
27 inhibitor Antimycin-A were made to measure mitochondrial response. All concentrations reported
28 are the final concentrations in each well.

29 **2.4 Mitochondrial respiration measurements via Orobos O2k respirometry:** Oxygen
30 consumption was determined using our established protocols (Alleman *et al.*, 2016). Immediately
31 after exposure to the PEFs, cells were centrifuged at 200 r.c.f. for 5 minutes. The cell pellet
32 obtained was re-suspended in an assay buffer (Buffer Z: 105mM K-MES, 30mM KCl, 10mM
33 KH₂PO₄, 5mM MgCl₂-6H₂O, 0.5mg/mL BSA, 20mM Creatine, 1mM EGTA, pH 7.1 in dH₂O).
34 Two milliliters of the cell suspension containing approximately 6 million cells was then transferred
35 to the Orobos O2k respiration chamber. A small volume from the sample was used to determine
36 cell number using a hemocytometer before transferring to the respiration chamber. The O2k
37 respiration chamber is equipped with calibrated oxygen measuring polarographic sensors. The
38 chamber was maintained at 37 °C, and the oxygen signals were allowed to stabilize before closing
39 the chamber to the outside air. After closing, the OCR was measured following no injections
40 (basal), 2 mM of malate and 10 mM glutamate (G/M), 5 mM of adenosine diphosphate (ADP),
41 and two injections of FCCP with a final chamber concentration of 0.3 μ M. All concentrations
42 reported are the final concentrations in each well. For control treatments in which the cells were
43 permeabilized using the chemical digitonin, OCR signals were allowed to stabilize after closing
44 the chamber following which digitonin (final concentration: 10 μ g/mL) was injected. The basal
45 rate was measured once the signals stabilized after digitonin injection. Measurements of the OCR
46 responses to G/M, ADP, and FCCP were as described above.

1 **2.5 Quantification of cell permeability using cell permeant Calcein:** Supernatant from cell
2 culture flasks (growth area: 75 cm²) was removed, and cells were washed with PBS^{-/-}. Following
3 the wash, growth media containing 5 µM cell permeant Calcein AM (ThermoFisher Scientific,
4 USA) was added to the flask (3 mL/75 cm²). After a thirty-minute incubation in a cell culture
5 incubator, cells were harvested following a standard Trypsin-EDTA harvesting procedure. Final
6 samples were placed in a 0.5 mL basal media, which was followed by treatment and immediate
7 centrifugation at 200 r.c.f. for 5 minutes. Samples were then placed on ice, and the supernatant
8 (100 µL) was collected at 10, 15, and 20 minutes. Fluorescence of Calcein was detected in the
9 supernatant using a spectrophotometer (BioRad, USA). The raw fluorescent unit (RFU) of controls
10 was monitored such that only those time-points at which the RFU of the control did not change
11 considerably were considered for measurements. The permeability was expressed as the fold
12 change of the RFU compared to the controls.

13 **2.6 Actin depolymerization using Latrunculin B:** Supernatant from cell culture flasks (growth
14 area: 75 cm²) was removed, and cells were washed with PBS^{-/-}. Following the wash, growth media
15 containing 1 µg/mL Latrunculin B (Sigma Aldrich, USA) was added to the flask. After a ten-
16 minute incubation in a cell culture incubator, the cells were checked under a microscope to verify
17 morphological changes. The supernatant was discarded, and cells were washed again with PBS^{-/-}.
18 Next, cells were harvested following a standard Trypsin-EDTA harvesting procedure.

19 **2.7 Statistical analyses:** The software JMP[®] (version 12, SAS Institute Inc., Cary, NC) was used
20 for statistical analyses. Samples were compared using a one-way analysis of variance (ANOVA)
21 followed by a post hoc Tukey HSD to find means that were significantly different from each other.

22 **3 RESULTS**

23 The effects of clinically-relevant µsPEFs on mitochondrial respiration was evaluated via high-
24 resolution respirometry. Briefly, cells in suspension were exposed to PEFs after which cells were
25 centrifuged and suspended in an assay buffer. The cell suspension volume of two milliliters was
26 transferred to the oxygraph chamber after which mitochondrial respiration response to the
27 substrates glutamate-malate, adenosine diphosphate, and protonophore carbonyl cyanide-p-
28 trifluoromethoxyphenylhydrazone (FCCP) was measured. A comparison of mitochondrial
29 responses between PEF and chemically induced (via Digitonin) permeabilizations of the cell
30 membrane was made. In addition, this investigation also probed into the significance of a nexus
31 between the actin cytoskeleton and the mitochondria.

32 **3.1 PEFs alone do not influence live cell mitochondrial membrane potential:** Cell suspensions
33 were exposed to electric field strengths (= applied voltage/distance between electrodes) of 600
34 V/cm, and 700 V/cm. The pulse duration was kept constant at 100 µs (see **Figure S1** in the
35 supplementary figure section), consistent with clinically used values (Martin II *et al.*, 2012;
36 Thomson *et al.*, 2011). The frequency of the electric fields was 1 Hz and the number of pulses 80.
37 These PEF parameters were not only chosen due to their clinical relevance but also due to our
38 previous observation of these field parameters influencing cell signaling in human and murine
39 triple negative breast cancer cells (Goswami *et al.*, 2017).

40 A preliminary analysis of the mitochondrial respiration of cells exposed to these PEFs was
41 made after allowing overnight incubation. Briefly, cells were exposed to PEFs and then seeded in
42 tissue culture Agilent XF Seahorse well plates. After overnight incubation, mitochondrial activity
43 was measured via oxygen consumption rates of cells in response to ATPase synthase inhibitor
44 oligomycin, uncoupling protonophore FCCP, and electron transport chain complex III inhibitor

1 Antimycin-A (**Figure 1A & 1B**). Two mitochondrial performance indices were calculated:
 2 respiratory reserve capacity and ATP production capacity. The respiratory reserve capacity is the
 3 difference between the OCRs as a response to uncoupling via FCCP and the basal rate. The
 4 protonophore FCCP collapses the mitochondrial membrane potential and is indicative of the
 5 maximum respiration the mitochondria can achieve. Respiratory reserve is a representative
 6 measure of the cell's ability to respond to increased metabolic demands. The OCR measured after
 7 inhibition of ATPase activity provides the fraction of basal rate involved in ATP production. Thus,
 8 the difference between the OCRs measured at the basal condition and after oligomycin injection
 9 provides a measure of the ATP production rate capacity of the cells.

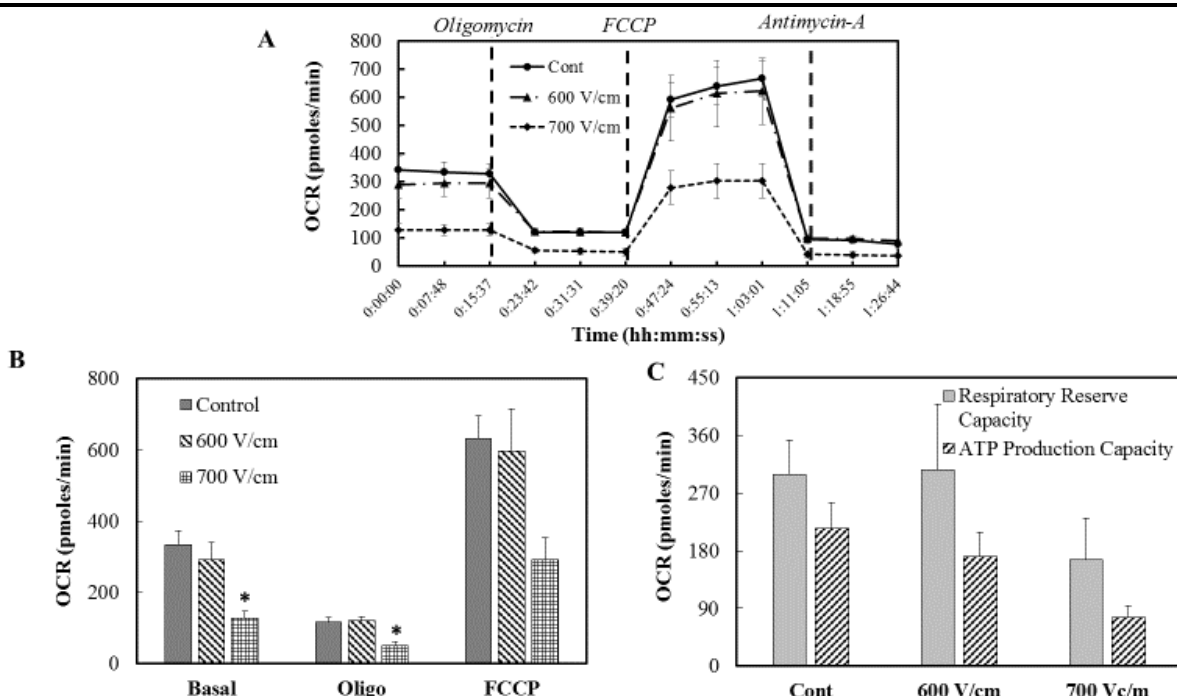


Figure 1: The OCR of live cell mitochondria after overnight incubation post PEF exposure (A). The OCR measurements expressed in pmoles/min are summarized in (B), and these measurements were used to calculate the respiratory reserve and ATP production capacities (C). One-way ANOVA analysis followed by a Tukey HSD post-test was performed to test for statistical significance. Error bars represent the standard error of the mean, and the number of sets per condition n = 3.

10 The XF metabolic data (**Figure 1C**) showed no difference in the respiratory reserve and ATP
 11 production capacities between the untreated controls and the cells exposed to 600 V/cm. There
 12 was a slight (albeit statistically insignificant) decrease in respiratory reserve capacity of cells
 13 exposed to 700 V/cm. Moreover, the ATP production capacity of cells exposed to 700 V/cm was
 14 lower than the untreated control, though statistically insignificant. Note that our previous
 15 measurements of cellular viabilities after overnight incubation (Goswami *et al.*, 2017) indicate that
 16 the live fraction of total cells, which survive exposure to PEFs, was determined to be
 17 approximately 80% and 40%, for 600 V/cm and 700 V/cm, respectively. This reduction in cell
 18 viability is consistent with the reduced absolute respiration rates in cells exposed to 700 V/cm seen
 19 in Figures 1B & 1C.

20 The XF metabolic data provided no conclusive evidence as to whether or not mitochondrial
 21 physiology is impacted by PEFs, since it could be argued that the differences in respiration can be

1 attributed to the fewer live cells in the 700 V/cm group versus the untreated controls. We next
 2 proposed that the impact of PEFs on mitochondrial respiration and physiology may only be limited
 3 to shorter temporal scales, i.e., immediately after exposure. To test this hypothesis, experiments
 4 using high-resolution respirometry were performed on cells exposed to PEFs. Mitochondrial
 5 responses to glutamate and malate (G/M), adenosine diphosphate (ADP), and protonophore FCCP
 6 were measured via the OCR normalized to live cells (pmoles/s-million units; **Figure 2A**). The
 7 glutamate-malate substrate partakes in the complex I activity of the electron transport chain (ETC)
 8 in the mitochondria whereby an electron is transferred forward through complexes III-IV. The
 9 electron flow is used in a series of reduction steps to convert molecular oxygen to water and
 10 establish a proton gradient across the mitochondrial membrane. The mitochondrial membrane
 11 potential is largely dependent on this proton gradient, and the proton gradient provides the free
 12 energy for the ATPase ‘turbines’ (Complex V) to phosphorylate ADP to the energy currency
 13 adenosine triphosphate (ATP). The responses to G/M and ADP, thus, provide a performance index
 14 of the ETC whereas the disruption of the proton gradient via FCCP collapses mitochondrial
 15 membrane potential.

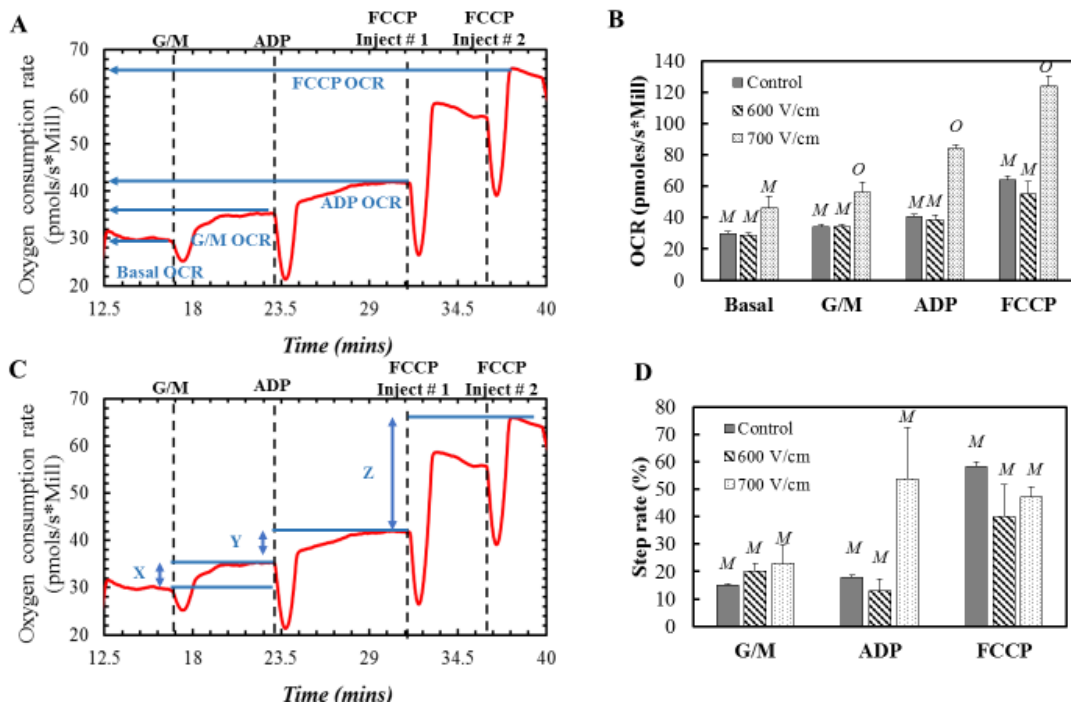


Figure 2: Representative oxygen consumption traces are shown in **Figures A** and **C** as references for **B** and **D**, respectively. The mitochondrial response to glutamate-malate (G/M), adenosine diphosphate (ADP), and FCCP was measured via oxygen consumption rates per million cells as shown in **B**. Another method of analysis is provided in terms of step heights of the metabolic profile in **C**. Error bars represent the standard error of the mean, and the number of sets per condition $n = 3$. Statistically non-distinct conditions were grouped by letter (e.g. M versus O) for each substrate response, to illustrate significant differences as determined by a one-way ANOVA followed by a Tukey HSD-post test. Note that the dips seen in the respirometry measurements (A & C) are due to disturbances created by the injections.

16 A representative respirometry plot is shown in **Figure 2A**. The initial equilibrated signal of the
 17 cell OCR was recorded as the basal rate. Respiration rates of cells were allowed to stabilize after

1 each injection of substrate/protonophore before making further injections. Two serial injections of
 2 FCCP were made and the highest response was recorded. Normalization of the OCR with live cells
 3 was performed by counting the approximate number of total cells via a hemocytometer and
 4 assuming the live fraction of the total count (Control: 100%; 600 V/cm: 80%; 700 V/cm: 40%)
 5 based on independent viability data we reported with the same cell and pulse conditions (Goswami
 6 *et al.*, 2017). Thus, the OCR was normalized and expressed in units of pmoles/s-million cells.
 7 Based on the experiments, it was observed that the untreated controls and the cells exposed to 600
 8 V/cm did not have significant differences in mitochondrial responses to G/M, ADP, and FCCP
 9 (**Figure 2B**). On the other hand, the cells exposed to 700 V/cm had significant differences with
 10 both the controls and the 600 V/cm group in all mitochondrial responses. The increased respiration
 11 rates after electric field exposure has been previously reported in isolated rat liver mitochondria
 12 (Reynaud *et al.*, 1989).

13 A source of error while reporting the normalized OCR is the variability in the total and live cell
 14 count. Thus, a normalization technique of the respirometry data independent of the live cell
 15 number was deemed useful in countering this variability. Moreover, the OCR after injection of a
 16 substrate/protonophore is dependent on the previous OCR step increments. To address these
 17 issues, a mathematical expression independent of the number of cells was used to isolate the
 18 individual step increments after each substrate injection. This step rate is defined as

$$\text{Step rate}_i = \frac{OCR_i - OCR_{i-1}}{OCR_{i-1}} \times 100 \quad \text{Eqn. 1}$$

19 In this expression, the subscript ‘*i*’ denotes a substrate (for e.g., ADP) and ‘*i-1*’ denotes the
 20 substrate used prior to ‘*i*’ (for e.g., *i-1* for ADP is G/M). Thus, graphically the G/M step rate is the
 21 height *X* (**Figure 2C**) divided by the basal OCR (**Figure 2A**) for the sample. Similarly, the ADP
 22 step rate is the height *Y* divided by the G/M OCR, and the FCCP step rate is the height *Z* divided
 23 by the ADP OCR. These fractions are expressed as percentages in **Figure 2D**. Moreover, the ratio
 24 in Eqn. 1 makes it independent of the number of live cells/mitochondrial mass in the sample. Based
 25 on this performance index, it is observed that the PEFs at 700 V/cm induce higher step increments
 26 in the G/M and ADP response although these are not statistically significant from the untreated
 27 controls (**Figure 2D**). Note, that individual recorded step-rate data for the ADP response in cells
 28 exposed to 700 V/cm was higher (31.9, 38.5, 91.2) than that for the controls (19.5, 17.4, 17.1), but
 29 possessed high variability due to which a strict statistical analysis would deem the two groups no
 30 different from each other. There are lower step increments in FCCP response in both treatment
 31 conditions (600 V/cm and 700 V/cm) but again not statistically significant. A lower step-increment
 32 could indicate the depolarization of the mitochondrial membrane. Thus, based on the data and
 33 within the range of micro-second PEF pulse parameters used, the mitochondrial membrane
 34 potential and physiology are not significantly altered.

35 **3.2 Chemical permeabilization of outer cell membrane leads to altered mitochondrial**
 36 **respiration:** Higher step rates for the G/M and ADP injections were recorded for cells exposed to
 37 the 700 V/cm PEF (**Figure 2**). A possibility exists that electric fields develop in the cytoplasmic
 38 cellular compartment because of permeabilization of the plasma membrane (Esser *et al.*, 2010),
 39 which, therefore, perturb the functioning of the voltage sensitive ETC. In addition, previous
 40 literature (Hamamoto *et al.*, 1982; Teissie, 1986) has reported increased ATP production in an
 41 isolated mitochondrion and bacterium when exposed to electric fields similar to those used in this
 42 study. However, an alternative explanation is perhaps that the permeabilization of the plasma
 43 membrane enhances trans-membrane substrate transport to the organelles.

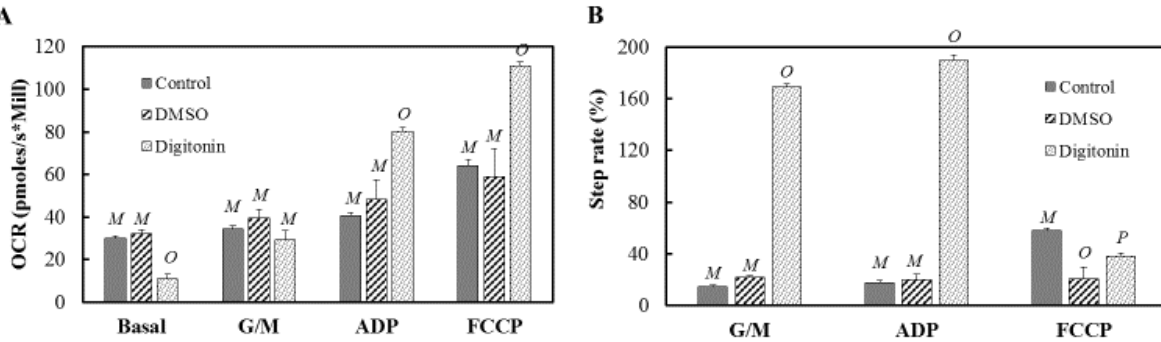


Figure 3: The OCR (A) and step rate (B) responses to different substrates are shown for cells without any treatment (control) and cells treated with DMSO and digitonin, respectively. Error bars are for the standard error of the mean, and $n = 3$ for the control and DMSO groups, while $n = 4$ for the digitonin group. Statistically non-distinct conditions were grouped by letter (e.g., M versus O versus P) for each substrate response, to illustrate significant differences as determined by a one-way ANOVA followed by a Tukey HSD-post test.

1 To clarify this issue, we quantified the permeability of cells exposed to PEF pulse parameters
 2 within the range used in this study. Briefly, cells were loaded with the cell permeant dye Calcein
 3 AM. The cell permeant dye is not fluorescent but is cleaved to release fluorescent cell impermeant
 4 Calcein upon internalization. After a thirty-minute incubation in a cell culture incubator followed
 5 by removal of any residual dye via wash steps with PBS, cells were harvested using Trypsin-EDTA
 6 solution and exposed to PEFs as detailed in the methods section. The stained cell sample was then
 7 centrifuged, and a pellet obtained (Figure S2). A volume of 100 μ L was drawn from the
 8 supernatant at 10, 15, and 20 minutes, and the fluorescence was read using a spectrophotometer to
 9 measure levels of Calcein. Fluorescence units were then normalized to untreated controls for a fold
 10 change in raw fluorescence units (RFU). Since the cell impermeant Calcein molecule is expected
 11 to leak out of permeabilized cells faster than out of the untreated controls, the fold change provides
 12 a semi-quantitative measure of cell permeability. A similar approach to measure cell permeability
 13 is reported by Neri *et al.* (2001). Note that although Calcein AM is typically used to measure cell
 14 viability, in the present investigation (as is done in Neri *et. al.*) it is only used to measure cell
 15 permeability. Based on the method described, the RFU fold change in PEF samples were
 16 approximately 2 for 600 V/cm and approximately 2.5 for 700 V/cm (Figure S2).

17 Next, digitonin detergent (Promega Corporation, USA) was used to permeabilize the cells and
 18 measure the mitochondrial response to the same substrates used for the PEF treatment group.
 19 Briefly, cells were placed in the oxygraph chamber and basal rates allowed to equilibrate. After
 20 equilibration, digitonin was injected to a final concentration of 10 μ g/mL. Again, the signal was
 21 allowed to equilibrate after which G/M, ADP, and FCCP were injected as in the case with the PEF
 22 treatment groups. Since the digitonin stock is supplied in a dimethyl sulfoxide (DMSO) solvent,
 23 an equal volume (1 μ L; final concentration 7 mM) of DMSO (Sigma Aldrich, USA) was also
 24 injected to measure changes due to the vehicle of the detergent. Note, the permeabilization due to
 25 the digitonin dosage was measured to be approximately 2 times higher than the untreated controls
 26 using the same approach as described above, i.e., the permeabilization was comparable to that
 27 observed for the PEF treated samples during the period of the Calcein release measurements.

28 Respirometry measurements were then carried out and are summarized in Figure 3. The plots
 29 illustrate OCR and step rate measurements for untreated cells (control) and cells exposed to DMSO
 30 and digitonin. The OCR measurements reveal that the digitonin significantly reduced the basal

1 rates in cells (**Figure 3A**) when compared to the control and DMSO population. Upon examining
2 the step rates (**Figure 3B**), the chemical permeabilization induces a higher G/M response, which
3 leads to an insignificant difference in the OCRs between the controls and the digitonin treated
4 groups (**Figure 3A**). The digitonin permeabilized cells have higher ADP responses when
5 compared to the other two populations (**Figures 3A and 3B**). A lower recovery was recorded, as
6 seen in the step rate data, for the chemically permeabilized cells when perturbed with FCCP
7 (**Figure 3B**). Thus, permeabilization via a non-electrical means also leads to increased responses
8 to the substrates and a reduced response with FCCP injection. An important distinction, however,
9 is the opposite directionality of the alteration in basal rates with the electrical and non-electrical
10 permeabilization and the much more pronounced G/M and ADP responses with the digitonin
11 permeabilization when the step-rate data was compared.

12 **3.3 Actin cytoskeleton and the mitochondrial nexus could dictate mitochondrial response to**
13 **PEFs:** The conflicting findings on the effects of PEFs on mitochondrial physiology in experiments
14 with intact cells versus isolated mitochondria leads to the question of whether or not there are
15 indirect secondary effects on the mitochondria due to alterations in other cellular structures. The
16 mitochondria are anchored onto the cell cytoskeleton in specialized cytoplasmic domains that
17 allow them to partake in regulatory and energetic processes. For example, mitochondrial
18 positioning in microdomains inside the cytoplasm allows calcium dependent mechano-sensing in
19 cardiac cells. For a review, the reader is directed to Schönleitner *et al.*, (2017). Aberrations in the
20 localization are implicated in disease. Thus, we next explored the possibility of alterations in the
21 mitochondrial membrane potential with PEFs following chemical alteration of the cytoskeleton.
22 Recent reports (Berghöfer *et al.*, 2009; Pakhomov *et al.*, 2014) have demonstrated that PEFs with
23 high magnitude electric field strengths (19-30 kV/cm; pulse width: order of ns; number of pulses:
24 1-4) cause structural damage to the cytoskeleton, including depolymerization of the actin structures
25 (Pakhomov *et al.*, 2014). We therefore hypothesized that an alteration in mitochondrial function
26 could be achieved with relatively low field strength PEFs (~700V/cm) after pre-treating the cells
27 with an actin depolymerizing agent.

28 To test this hypothesis, cells were treated with Latrunculin B (LanB) to depolymerize the actin
29 cytoskeleton. The LanB forms a complex with the globular (G)-actin monomer and prevents the
30 polymerization to filamentous (F)-actin (Morton *et al.*, 2000). Briefly, cells were treated with 1
31 μ g/mL LanB for 10 minutes. Fixed staining of the cells with the Alexa Fluor Phalloidin conjugate
32 (ThermoFisher Scientific, USA) for F-actin and the nuclear dye DAPI (Sigma Aldrich, USA)
33 demonstrated that the dosage of LanB for 10 minutes was sufficient to compromise the F-actin
34 structures of the 4T1 cells (**Figure 4A**). Following incubation with LanB, cells were washed with
35 PBS^{-/-} to make sure no residual drug remained. Cells were then harvested and exposed to a PEF at
36 700 V/cm immediately after which respirometry measurements were made as described in the
37 previous sections. Note that an applied field of 700 V/cm does not imply an equivalent electric
38 dosage between those treated with LanB and those that were not. Furthermore, the cell size directly
39 impacts the influence of the electric field on the plasma membrane (Goswami *et al.*, 2017;
40 Schoenbach *et al.*, 2007), and, therefore, cell size measurements were made. Both untreated
41 controls and LanB treated cells had a comparable mean diameter. A probability density function
42 of the sizes is provided for reference in **Figure S3**. However, one cannot rule out the impact that
43 LanB may have on other lipid reorganization events which may impact the electric field sensed by
44 the cell across the membrane. Since the LanB stock was prepared in DMSO solvent, respirometry
45 was performed on cells incubated with a volume of the vehicle (final concentration 14 mM) equal
46 to that of the LanB. Note that the OCR data normalized to live cells is not provided for this section

1 of the study due to challenges in determining live cell fractions immediately after administration
 2 in combinatorial treatments involving PEFs. The challenges are discussed in the section that
 3 follows. The step rates obtained from the respirometry measurements are shown in **Figure 4B**.
 4 The step rate data of untreated cells (control) and vehicle DMSO are provided for reference.

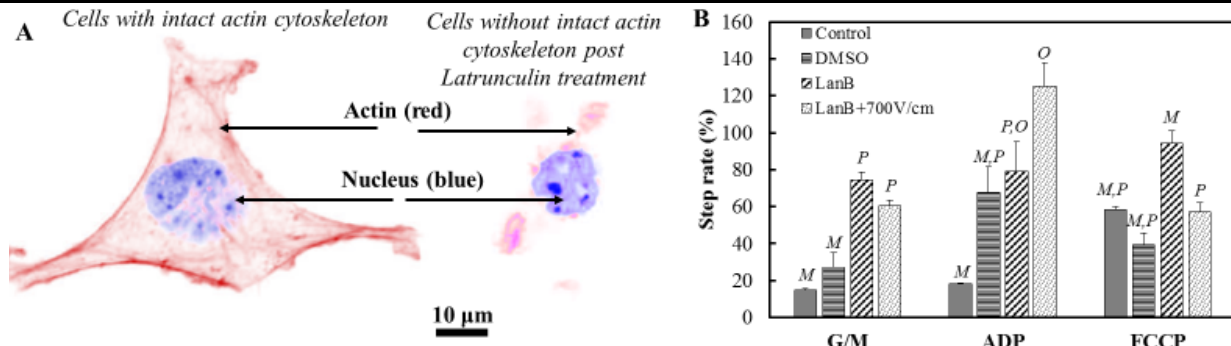


Figure 4: Treatment with Latrunculin B compromises the actin cytoskeleton as shown in the fixed cell staining image (A) of the actin (red) and the nucleus (blue). A 10 μ m scale bar is shown. Shown in B is the step rate data for cells with no treatment (control), those treated with the Lan B vehicle DMSO, those treated with Lan B, and those with PEF exposure post the Lan B treatment. The error bars represent the standard error of the mean, and the sample size per set is $n = 3$ for all except the LanB+700V/cm ($n=4$) treatment. Treatment conditions connected by different letters (M, O, and P) within each substrate response are statistically different as determined by a one-way ANOVA followed by a Tukey HSD-post test.

5 The step rate data (**Figure 4B**) suggests that treatment with LanB leads to an increased G/M
 6 response when compared with untreated controls and cells treated with vehicle DMSO. Upon
 7 exposure to a PEF field of 700 V/cm, cells compromised of their actin cytoskeleton via LanB
 8 treatment did not significantly differ in their G/M and ADP responses when compared to cells
 9 treated with LanB alone. However, actin disruption and PEF exposure reduced the response of
 10 cells to FCCP when compared to cells only treated with actin depolymerizing agent LanB. Thus,
 11 the step rate data suggests that relatively low field strength PEFs can impact the mitochondrial
 12 membrane potential upon depolymerization of the actin as seen by the comparison of the FCCP
 13 responses between LanB and LanB+700V/cm groups (**Figure 4B**).

14 4 DISCUSSION

15 In this study, murine triple negative breast cancer 4T1 cells were exposed to PEF parameters
 16 typically used in a clinical setting. The pulse train used consists of 80 to 100 pulses each with a
 17 100 μ s width applied at a frequency of 1 Hz. Note that this clinical modality is also known by the
 18 names of irreversible electroporation (IRE) or Nanoknife. The cells were exposed to these μ sPEFs
 19 and the mitochondrial states measured via either an Agilent Seahorse machine or high resolution
 20 respirometry to determine whether or not these types of microsecond pulses significantly alter
 21 mitochondrial physiology.

22 As a first step, this investigation measured the mitochondrial respiration in cells exposed to 80
 23 μ sPEF pulses with amplitudes of 600 and 700 V/cm and incubated overnight. The rationale of
 24 choosing these field strengths is two fold. First, there is an immediate severe loss of viability of
 25 4T1 cells at field strengths above 700 V/cm. Thus, an understanding about mitochondrial
 26 alterations is lost at these higher strengths due to the damage experienced by the entire cell. Second,
 27 it has recently been demonstrated that at field strengths of 600 and 700 V/cm the μ sPEF pulse train

1 induces cell signaling alterations in both murine and human breast cancer cells towards a less
2 immunosuppressive inflammatory state as determined by the reduction of thymic stromal
3 lymphopoietin (TSLP) signaling (Goswami *et al.*, 2017). The measurements of mitochondrial
4 respiration after overnight incubation were performed using an Agilent Seahorse machine. Note
5 that it is not necessary for the mitochondrial physiology in surviving cells to remain similar to the
6 controls. For example, Zhang *et al.* (2014) reported mitochondrial hyperpolarization in viable cells
7 24 hours after treatment with a drug. Given that the cells that escape μ sPEFs had altered cell
8 signaling as reported by Goswami *et al.* (2017), the objective of this investigation was to determine
9 if alterations in mitochondrial respirations are also observed in cells that survive μ sPEFs when
10 compared to untreated controls. The data (**Figure 1**) gathered in the present investigation suggests
11 that there are no significant alterations in the mitochondrial physiology in the cells that escape or
12 recover from the μ sPEF treatment. This finding is in agreement with that reported by Estlack *et*
13 *al.* (2014a), who used an almost identical Seahorse protocol and found no alterations in
14 mitochondrial respiration in Jurkat and U937 cells exposed to nsPEFs and allowed to recover over
15 a period ranging from an hour up to as long as 24 hours after exposure. Thus, it may be supposed
16 that the effects of these types of nsPEF and μ sPEFs on mitochondrial respiration, if any, are short
17 lived (i.e., below one hour).

18 To test whether or not mitochondrial perturbations exist immediately after μ sPEF exposure,
19 the mitochondrial respiration of 4T1 cells was measured in the present study promptly after
20 treatment with the aforementioned field strengths using high resolution respirometry. Cell
21 response to injections of G/M and ADP were made to probe the state of the electron transport chain
22 (ETC). The changes in oxygen consumption rate (OCR) in response to G/M reflect alterations in
23 the complex I activity of the ETC whereas ADP responses provide a measure of the cell's capacity
24 to produce ATP. A final injection of FCCP was made to measure the maximal mitochondrial
25 respiration. When comparing the responses of control and treatment groups to FCCP, a lowered
26 response in one implies a smaller proton gradient across the mitochondrial membrane and,
27 therefore, a lower mitochondrial potential compared to another group. The OCR data are
28 dependent on the mitochondrial mass/number, and, thus, in this investigation, the OCR is
29 normalized to an estimate of the number of live cells based on independent measurements. To
30 circumvent the artifacts that may be introduced due to this cell number and mitochondrial mass
31 dependence, the data is also presented as step rates, whereby an automatic normalization is made
32 within the sample. Such a step-rate approach is very similar in nature to how data using fluorescent
33 dyes to measure mitochondrial membrane potential are reported where the alteration in membrane
34 potential is measured in terms of changes in the fluorescent units before and after a treatment.

35 **4.1 Summary of the respirometry data and a comparison with the literature:** In this
36 investigation, the respirometry measurements on cells exposed to μ sPEF show increased basal
37 OCR rates 55% higher (albeit statistically not significant) for field strength of 700 V/cm when
38 compared to the untreated controls (**Figure 2B**). Increases in the normalized OCR data were also
39 observed in G/M (63%), ADP (107%), and FCCP (93%) responses for the μ sPEF-exposed
40 population when compared to the untreated controls ($p<0.05$). Conversely, while the step-rate
41 response changes measured were not statistically significant, the trends were that while the G/M
42 and ADP responses in the μ sPEF treated cells increased when compared to the controls, the FCCP
43 response was 18% lower. To explain these respiration responses, we next considered the enhanced
44 permeabilization of the outer membrane that we independently measured for the 600 and 700 V/cm
45 conditions (**Figure S2**). Based on the existing literature, a number of plausible scenarios may be
46 responsible for these response alterations due to outer cell membrane permeabilization. They are

1 discussed below.

2 A first scenario is that the permeability of the cell's outer membrane promotes an unhindered
3 flow of ions and substrates from the extracellular compartment, thereby leading to an increase in
4 respiration due to both G/M and ADP more easily reaching the mitochondria. To recreate this
5 scenario in our experiments, we used a chemical agent digitonin that specifically permeabilizes
6 the outer cell plasma membrane without affecting the nuclear envelope (Griffis *et al.*, 2003; Tissera
7 *et al.*, 2010). The digitonin permeabilized cells showed decreased basal rates when compared to
8 the untreated controls (**Figure 3A**), which Vercesi *et al.* (1991) claim may be due to a reduction
9 in the adenine nucleotides resulting in a non-phosphorylating state of the mitochondria. Due to
10 the lower basal rates initially, the G/M response of the digitonin-permeabilized cells was lower by
11 14% for the normalized OCR data when compared to the G/M response of the untreated controls.
12 The analysis of step rate data (**Figure 3B**), however, provides a clearer picture, showing an
13 increased respiration (> 10 fold compared to the controls) in response to the G/M and ADP
14 injections in the digitonin-permeabilized cells. While the G/M and ADP responses can be
15 explained due to an unhindered flow of substrates into the cell, the question, nonetheless, arises as
16 to how the mitochondria may be depolarized, as measured by the FCCP response, due to the
17 permeabilization of the cell's outer membrane? In our study, a significant decrease in FCCP step-
18 rate response was recorded in the digitonin-permeabilized cells when compared to the control,
19 suggesting an impact on the mitochondrial membrane potential. Previous measurements on
20 isolated mitochondria of their electrical properties by Pauly *et al.* (1960) and Schwan (1959) show
21 an almost linear dependence of the internal conductivity of the mitochondria on changes in the
22 external ionic concentrations. Of course, this relationship may not be linear in live-cell
23 mitochondria. Nonetheless, an alteration in the cytoplasmic ionic concentrations due to the
24 permeabilization of the cell's outer membrane and resulting changes in the electrical properties of
25 the mitochondria would be consistent with the FCCP responses we report.

26 A second scenario is that exogenous electric fields, which gain access into the cell's interior
27 after outer membrane permeabilization, directly affect the mitochondria, contributing to our
28 observed increases in respiration at 700 V/cm. Based on the existing literature, it is thought that
29 an exogenous electric field can either lead to an increase in ATP production by the mitochondria
30 or lead to an alteration in the mitochondrial physiology (i.e., via mitochondrial membrane
31 permeabilization and/or fusion). In experiments conducted by Hamamoto *et al.* (1982), isolated rat
32 liver mitochondria were exposed to PEFs with pulse widths ranging from 100 μ s to 10 ms at
33 intervals of 30 s. Hamamoto *et al.* reported an increase in ATP synthesis in the mitochondria upon
34 exposure to the PEFs as measured via esterification of the radioactive inorganic phosphate.
35 Moreover, the production increased with increases in both the pulse number and field strengths (>
36 400 V/cm). In their work, the authors claim that the reason for the increase in ADP to ATP turnover
37 with electric fields is due to the artificially imposed ion gradients across the mitochondrial
38 membrane, thus influencing the membrane potential. In addition, they noted that disruption of the
39 mitochondrial membrane potential via FCCP injection disabled the influence of the electric field
40 in stimulating ATP production. This observation of reduced ATP production in the compromised
41 mitochondria of *Escherichia coli* bacteria exposed to μ sPEFs has also been reported elsewhere
42 (Teissie, 1986). Therefore, based on this literature, as long as the mitochondrial membrane
43 potential does not decrease due to the presence of the electric field, an increase in ATP turnover is
44 possible.

45 Yet another scenario is that indirect effects on the mitochondria due to a cell's outer membrane
46 permeabilization may occur via alterations in other cellular structures. The disruption of cell

1 homeostasis due to permeabilization could lead to cell swelling and as a result stress the cell
2 cytoskeleton. For example, actin disassembly due to outer cell permeabilization and cell-swelling
3 was reported by Pakhomov *et al.* (2014) when CHO-K1 cells were exposed to nsPEFs (600 ns
4 pulse widths, 2 Hz frequency, ~20 kV/cm). Two other investigations (Berghöfer *et al.*, 2009;
5 Hohenberger *et al.*, 2011) in the literature report actin disassembly in plant cells exposed to
6 nsPEFs. However, these latter reports only mention cell permeabilization and not cell swelling. To
7 explore the direct impact of actin disassembly on mitochondrial respiration, we used the drug LanB
8 to depolymerize the actin cytoskeleton. Once the actin network was compromised, the cells were
9 exposed to μ sPEF fields of 700 V/cm. The step-rate data (**Figure 4B**) sheds light on how low-
10 level fields (i.e., low-level when compared to the ~kV/cm fields used by the studies above) can
11 impact the mitochondrial membrane potential once the actin cytoskeleton, on which the
12 mitochondria are anchored, is compromised. It is noted that Thompson *et al.* (2014) demonstrated
13 that treatment with Latrunculin A altered cell membrane rigidity in CHO cells making them more
14 susceptible to nsPEF pulses of 150 kV/cm. However, it is difficult to draw specific conclusions
15 regarding the details of mitochondrial effects from the Thompson *et al.* data. In contrast, the
16 present investigation, a link is provided between actin dynamics and the susceptibility of the
17 mitochondria to μ sPEF using detailed mitochondrial respirometry experiments. Although the
18 specific mechanism remains to be explored in future work, a hypothesis may be derived as to why
19 actin depolymerization may impact mitochondria more when exposed to μ sPEF based on the
20 existing literature. Actin filament dynamics play an important role in apoptotic pathways (Desouza
21 *et al.*, 2012) such as anoikis. The pro-apoptotic protein Bmf can translocate from the myosin V
22 actin motor complex to the mitochondria in the event of activation of anoikis and neutralize the
23 anti-apoptotic protein Bcl-2 (Puthalakath *et al.*, 2001). It has also been demonstrated that activation
24 of the caspase cascade leads to fragmentation of the actin cytoskeleton into 31 kDa Fractin and 14
25 kDa tActin. Transfection of tActin into mammalian cells results in morphological alterations (for
26 example, cell rounding) associated with apoptosis, indicating a role for actin fragmentation in
27 downstream caspase signaling pathway (Mashima *et al.*, 1997, 1999). In addition to acting as a
28 substrate for the caspase pathway, actin cytoskeleton dynamics can also initiate caspase signaling
29 via both extrinsic and intrinsic apoptotic pathways. For example, CD95/FasL mediated apoptosis
30 was shown to be dependent on the interaction between the actin associated ezrin protein and FasL
31 (Parlato *et al.*, 2000). On the other hand, changes in the actin filament dynamics via point mutations
32 in the yeast actin isoform have been shown to induce the accumulation of reactive oxygen species
33 (ROS) and mitochondrial membrane depolarization involved in intrinsic apoptotic pathways
34 (Gourlay *et al.*, 2004). Alteration in the actin filament dynamics brought about by treatment with
35 the drug family Latrunculin and Cytochalasin D have been shown to induce the translocation of
36 pro-apoptotic Bcl-2 proteins to the mitochondria and induce mitochondrial depolarization. In
37 addition, experiments on *Arabidopsis* root hair treated with LanB conducted by Wang *et al.* (2010)
38 reveal that actin disruption leads to an opening of the mitochondrial permeability transition pore
39 which in turn results in a surge in calcium release by the mitochondria. Calcium imbalance in the
40 cytoplasm can alter mitochondrial physiology. It has also been noted that fragmentation into tActin
41 is thought to induce an apoptotic positive feedback loop via cleavage of the pro-apoptotic protein
42 Bid (Slee *et al.*, 2000). The nearly 40% reduction in OCR we observe in response to FCCP
43 injection in the μ sPEF-treated cells (LanB + 700 V/cm; **Figure 4B**) when compared to the controls
44 (LanB) would be consistent with mitochondrial membrane potential changes enhanced due to actin
45 disruption. Remarkably, Estlack *et al.* (2014b) demonstrated that nsPEFs can modulate extrinsic-
46 mediated apoptotic pathways via the CD95/Fas receptor, although intrinsic pathways involving

1 the mitochondria were unaffected. Thus, there remains a largely unexplored area of actin-
2 mitochondria-cell membrane nexus interactions that may dictate PEF sensitivity of cancerous cells
3 providing a promising avenue for future work.

4 In the context of these three scenarios and keeping in mind that the present investigation
5 observed neither a drastic decrease in FCCP response nor a drastic increase in ADP turnover in
6 cells exposed only to μ sPEFs (**Figure 2**), *it may be concluded that mitochondrial membrane*
7 *potential and physiology are not drastically altered by the μ sPEF pulse parameters used here.*

8 Note that the effect of substrates and inhibitors (i.e., G/M, ADP, FCCP, etc.) depend on the
9 sequence in which they are applied in an experimental study. Therefore, the relative changes in
10 mitochondrial membrane potential reported in this study are relative changes between two
11 treatments and not absolute values. While the effects of the sequence of substrates and inhibitors
12 was not explored here, mechanistic computational models of mitochondrial bioenergetics
13 combined with the results from the present investigation can guide the formulation of future
14 hypotheses. One such class of computational frameworks uses thermodynamic flux-force
15 relationships to model the coupled transport of mass and charge across the mitochondrial
16 membrane and, thus, predict the influence that each flux-force term (for example, the flux of Ca^{2+}
17 across the membrane) can have on the kinetics of mitochondrial membrane potential (Beard, 2005;
18 Bertram *et al.*, 2006; Magnus and Keizer, 1997). Integration of such models with experimental
19 studies have teased out many interesting facets of the link between mitochondrial bioenergetics
20 and apoptosis. For example, Huber *et al.* (2011) demonstrated that increased glycolysis by
21 cancerous cells generated ATP that supported flux reversal of the ATP synthase and thereby
22 repolarizing the mitochondrial membrane potential even in the presence of the adverse conditions
23 normally associated with cell death (cytochrome c release). Such repolarizations allow the
24 cancerous cells to escape apoptotic events. This highlights the need to investigate the role of the
25 tumor microenvironment, changes in cellular glycolytic capacity, as well as different phenotypes
26 of cells on mitochondrial response to μ sPEFs.

27 Our studies provide interesting insight into the bioenergetic responses following two different
28 approaches to acutely permeabilize the plasma membrane (using μ sPEF and Digitonin). Both
29 methods lead to similar cellular rates of ADP- and FCCP-dependent respiration, with each
30 treatment roughly doubling the OCR rate compared to the respective control (Figures 2B and 3A).
31 These data suggest that the *acute* treatment with detergent or PEF is not leading to drastic
32 alterations in mitochondrial membrane potential or ATP-generating capacity by the respiratory
33 chain. These findings are in contrast to our studies after overnight incubation post-PEF exposure,
34 where 700V/cm tended to decrease (albeit not statistically significantly) mitochondrial energetics.
35 It seems plausible that acute buffering of cellular ATP pools by glycolysis may sustain energetics
36 during the acute stressors (as described in Huber *et al.* (2011)), but that this buffering capacity may
37 have been exhausted after overnight incubation. There are also interesting differences in
38 mitochondrial energetics between acute permeabilization and acute μ sPEF, notably the large step
39 changes after the addition of glutamate/malate and ADP (in Digitonin compared to μ sPEF). We
40 cannot rule out that paradigm-specific differences in the extent/duration of plasma membrane
41 permeabilization led to a cellular “wash-out” of endogenous co-factors that influenced basal and
42 glutamate/malate-mediated respiration, which may explain the variance observed following the
43 detergent treatment. Future studies to further probe these ideas, perhaps in conjunction with
44 studies using computational models (Beard (2005); Bertram *et al.*, (2006); Magnus and Keizer,
45 1997)), should advance our understanding of the similarities and differences among these models.

1 However, an important finding in our investigation with implications for the use of PEFs (or
2 IRE/Nanoknife) in cancer therapeutics is that of the relationship between the actin networks and
3 mitochondrial physiology. This is discussed in the following.

4 **4.2 Implications for cancer therapeutics:** The clinical site of PEF (or IRE/Nanoknife) delivery
5 in tissue experiences a heterogeneous field leading to both lethal and sub-lethal zones. While lethal
6 zones are defined by complete cell death in the region of high electric field exposure, sub-lethal
7 zones experiencing low-level electric fields persist around the tumor margin where malignant cells
8 may exist. Moreover, the treatment zone is limited in volume by a tradeoff between the high
9 electric field magnitudes required to kill cells (~1000 V/cm) and the magnitude of fields that may
10 be safely delivered clinically without inducing deleterious side effects such as muscle contractions.
11 It would, therefore, be highly advantageous to be able to increase the tumor treatment volume
12 and/or induce changes in cell signaling towards an anti-tumor phenotype within a larger sub-lethal
13 treatment volume (Goswami *et al.*, 2017). To do so, chemo or molecular targeted therapies can be
14 leveraged in conjunction with PEF exposure as is done in electrochemotherapy (ECT) (Kunte *et*
15 *al.*, 2017; Plaschke *et al.*, 2017) to target sub-lethal zones. For example, exposure of 3D spheroids
16 to both PEFs and calcium has been shown to specifically inhibit the growth of tumorous cells
17 rather than healthy fibroblasts (Frandsen *et al.*, 2015). Similar pulse parameters as in the present
18 investigation have been used to make glioblastoma cells more susceptible upon PEF exposure
19 combined with calcium loading (Wasson *et al.*, 2017). Ivey *et al.* (2017) recently reported that
20 cancerous cells were specifically killed by PEFs over healthy cells upon induction of cell
21 morphological changes brought about via molecular targeting of the EphA2 receptor on human
22 glioblastoma cells. Our current study suggests that molecular adjuvants targeting actin
23 cytoskeleton could be used in conjunction with PEFs to induce cellular death even with low-
24 strength electric fields by further perturbing the organelles such as the mitochondria. While high-
25 strength electric fields (60-300 kV/cm) have been known to cause damage to the actin cytoskeleton
26 and DNA fragmentation leading to cell death (Stacey *et al.*, 2003, 2011), molecular adjuvants such
27 as LanB may enhance the kill zone even at low electric field strengths such as those used in our
28 investigation. However, a mechanistic view must be derived to understand the synergistic effects
29 of actin cytoskeleton disruption and PEFs on mitochondrial respiration and the promotion of cell
30 death.

31 In this regard, several mechanisms by which LanB and related molecules may induce cell death
32 are relatively well documented. Treatment with LanB, in the range from 0.01 to 10 μ M, for 10
33 minutes has been reported to cause DNA fragmentation leading to programmed cell death in pollen
34 cells when assessed 8 hours after treatment (Thomas *et al.*, 2006). In human gastric carcinoma
35 cells, treatment with Latrunculin A (LanA) led to increased caspase-3/7 activity when assessed 24
36 hours after treatment. Treatment of these cells with concentrations between 1-10 μ M led to cell
37 viabilities in the range of 20-60% (Konishi *et al.*, 2009). Another study on human breast cells
38 found that treatment with LanA led to cleavage of the poly (ADP-ribose) polymerase protein
39 involved in DNA damage repair (Martin and Leder, 2001). It would, therefore, be reasonable to
40 assume that the combination of LanB to disrupt the actin cytoskeleton and PEF exposure would
41 induce a higher cell death rate than the separate treatments alone.

42 It is worth noting that there are important remaining open questions for future work. A report
43 by Xiao *et al.* (2011) demonstrated outcomes that at first do not seem clearly reconciled with those
44 that we report here. In their study, Xiao *et al.* exposed human liver cancer cells, pretreated with an
45 actin-depolymerizing drug Cytochalasin B, to nsPEFs (450 ns pulse widths delivered at a
46 frequency of 1 Hz and 8 kV/cm). For their measurements of cell death, Xiao *et al.* used the fact

1 that cells in the early stages of cell death translocate a protein phosphatidylserine from the inner
2 leaflet of the cell membrane to the outside. This expression of the protein on the cell outer
3 membrane can be detected via Annexin V staining. Surprisingly, Xiao *et al.* report that cells with
4 disrupted actin networks and exposed to PEFs had a reduced percentage of the population
5 expressing this protein when compared to PEFs alone. The reason for this observation is not
6 understood, although it may be noted that Annexin V staining on cells performed immediately
7 after PEF permeabilization may provide false positives since the molecule Annexin V may be able
8 to access the interior of the cell due to cell membrane permeabilization caused by the PEF. The
9 primary reason for cellular death with PEFs is hypothesized to be the loss of homeostasis due to a
10 compromised outer membrane. However, the exact mechanism of cellular death caused by PEFs
11 is still debated (Deipolyi *et al.*, 2014; Maček-Lebar and Miklavčič, 2001). The potential for
12 reversible permeabilization of cells, in which cells recover from the loss of homeostasis, due to
13 PEFs also makes it difficult to ascertain live cell populations using simple dyes such as Trypan
14 Blue immediately after PEF treatment. However, we are hopeful that new cancer therapy insights
15 will result from identifying the specific mechanisms regulating cellular responses to combinatorial
16 treatments such as those we investigate here.

17 5 CONCLUSION

18 There is a limited understanding of whether or not μ sPEFs based on the IRE/Nanoknife clinical
19 treatment modality directly impact the cell mitochondrial physiology of the treatment zone. To
20 address this gap in knowledge, the present investigation provides measurements of the
21 mitochondrial state via high resolution respirometry on 4T1 cells exposed to μ sPEF pulse trains
22 that are used in clinical settings. In these measurements, the ETC state of the mitochondria is
23 probed via responses to G/M and ADP. Additionally, changes in the mitochondrial membrane
24 potential are inferred via responses to FCCP. It is observed in the present study that the impact of
25 μ sPEFs on mitochondrial respiration is short (< 1 hour) and temporary. Moreover, it is proposed
26 here that these alterations are primarily due to the permeabilization of the cell's outer (plasma)
27 membrane. Comparison between responses of cells exposed to μ sPEFs versus the chemical
28 permeabilization agent digitonin indicates that clinically used μ sPEFs do not significantly alter
29 mitochondrial physiology within the pulse parameters tested. However, our finding of the
30 mitochondria's susceptibility to sub-lethal μ sPEFs when the cell's actin cytoskeleton is
31 compromised via the actin depolymerizing agent LanB could provide both mechanistic insights as
32 well as avenues for increasing the IRE/Nanoknife treatment volume in a clinical setting.

33 AUTHOR CONTRIBUTIONS

34 I.G.: study design, cell culture, respirometry experiments, data analysis and interpretation, and
35 writing of manuscript; J.B.P: design of O2k experiments, and writing of manuscript; M.A.A: design of XF Seahorse experiments, and writing of manuscript; D.A.B.: data analysis and
36 interpretation, and writing of manuscript; M.R.v.S.: conception of project plan and study design,
37 data analysis and interpretation, and writing of manuscript; S.S.V.: conception of project plan and
38 study design, data analysis and interpretation, and writing of manuscript.
39

41 ACKNOWLEDGEMENTS

42 Goswami was funded by a Computational Tissue Engineering Fellowship offered by the Virginia
43 Tech Interdisciplinary Graduate Education Program. Allen received a research fellowship from

1 the Translational Obesity Research Program of the Virginia Tech Interdisciplinary Graduate
2 Education Program. This work was supported by the National Cancer Institute of the National
3 Institutes of Health through awards R01CA213423 and R01 HL123647, and by a National
4 Science Foundation CAREER Award (CBET-1652112).

5

6 REFERENCES

7 Alleman, R.J., Tsang, A.M., Ryan, T.E., Patteson, D.J., McClung, J.M., Spangenburg, E.E., Shaikh, S.R.,
8 Neufer, P.D., and Brown, D.A. (2016). Exercise-induced protection against reperfusion arrhythmia
9 involves stabilization of mitochondrial energetics. *Am. J. Physiol.-Heart Circ. Physiol.* **310**, H1360–H1370.

10 Beard, D.A. (2005). A biophysical model of the mitochondrial respiratory system and oxidative
11 phosphorylation. *PLoS Comput. Biol.* **1**, e36.

12 Beebe, S.J., Fox, P.M., Rec, L.J., Willis, E.L.K., and Schoenbach, K.H. (2003). Nanosecond, high-intensity
13 pulsed electric fields induce apoptosis in human cells. *FASEB J. Off. Publ. Fed. Am. Soc. Exp. Biol.* **17**,
14 1493–1495.

15 Berghöfer, T., Eing, C., Flickinger, B., Hohenberger, P., Wegner, L.H., Frey, W., and Nick, P. (2009).
16 Nanosecond electric pulses trigger actin responses in plant cells. *Biochem. Biophys. Res. Commun.* **387**,
17 590–595.

18 Bertram, R., Gram Pedersen, M., Luciani, D.S., and Sherman, A. (2006). A simplified model for
19 mitochondrial ATP production. *J. Theor. Biol.* **243**, 575–586.

20 Chandel, N.S. (2014). Mitochondria as signaling organelles. *BMC Biol.* **12**, 34.

21 Dai, W., Cheung, E., Alleman, R.J., Perry, J.B., Allen, M.E., Brown, D.A., and Kloner, R.A. (2016).
22 Cardioprotective Effects of Mitochondria-Targeted Peptide SBT-20 in two Different Models of Rat
23 Ischemia/Reperfusion. *Cardiovasc. Drugs Ther.* **30**, 559–566.

24 Deipolyi, A.R., Golberg, A., Yarmush, M.L., Arellano, R.S., and Oklu, R. (2014). Irreversible
25 electroporation: evolution of a laboratory technique in interventional oncology. *Diagn. Interv. Radiol.* **20**,
26 147–154.

27 Desouza, M., Gunning, P.W., and Stehn, J.R. (2012). The actin cytoskeleton as a sensor and mediator of
28 apoptosis. *Bioarchitecture* **2**, 75–87.

29 Esser, A.T., Smith, K.C., Gowrishankar, T.R., Vasilkoski, Z., and Weaver, J.C. (2010). Mechanisms for the
30 intracellular manipulation of organelles by conventional electroporation. *Biophys. J.* **98**, 2506–2514.

31 Estlack, L., Roth, C., Cerna, C., J. Wilmink, G., and Ibey, B. (2014a). Investigation of a Direct Effect of
32 Nanosecond Pulse Electric Fields on Mitochondria. *Proc. SPIE* **8941**.

33 Estlack, L.E., Roth, C.C., Thompson, G.L., Lambert, W.A., and Ibey, B.L. (2014b). Nanosecond pulsed
34 electric fields modulate the expression of Fas/CD95 death receptor pathway regulators in U937 and
35 Jurkat Cells. *Apoptosis* **19**, 1755–1768.

1 Frandsen, S.K., Gibot, L., Madi, M., Gehl, J., and Rols, M.-P. (2015). Calcium Electroporation: Evidence for
2 Differential Effects in Normal and Malignant Cell Lines, Evaluated in a 3D Spheroid Model. *PLOS ONE* 10,
3 e0144028.

4 Goswami, I., Coutermash-Ott, S., Morrison, R.G., Allen, I.C., Davalos, R.V., Verbridge, S.S., and Bickford,
5 L.R. (2017). Irreversible electroporation inhibits pro-cancer inflammatory signaling in triple negative
6 breast cancer cells. *Bioelectrochemistry* 113, 42–50.

7 Gourlay, C.W., Carpp, L.N., Timpson, P., Winder, S.J., and Ayscough, K.R. (2004). A role for the actin
8 cytoskeleton in cell death and aging in yeast. *J. Cell Biol.* 164, 803.

9 Griffis, E.R., Xu, S., and Powers, M.A. (2003). Nup98 localizes to both nuclear and cytoplasmic sides of
10 the nuclear pore and binds to two distinct nucleoporin subcomplexes. *Mol. Biol. Cell* 14, 600–610.

11 Hamamoto, T., OHNO, K., and KAGAWA, Y. (1982). Net Adenosine Triphosphate Synthesis Driven by an
12 External Electric Field in Rat Liver Mitochondria. *J. Biochem. (Tokyo)* 91, 1759–1766.

13 Hohenberger, P., Eing, C., Straessner, R., Durst, S., Frey, W., and Nick, P. (2011). Plant actin controls
14 membrane permeability. *Biochim. Biophys. Acta BBA - Biomembr.* 1808, 2304–2312.

15 Huber, H.J., Dussmann, H., Kilbride, S.M., Rehm, M., and Prehn, J.H.M. (2011). Glucose metabolism
16 determines resistance of cancer cells to bioenergetic crisis after cytochrome-c release. *Mol. Syst. Biol.* 7,
17 470.

18 Ivey, J.W., Latouche, E.L., Sano, M.B., Rossmeisl, J.H., Davalos, R.V., and Verbridge, S.S. (2015). Targeted
19 cellular ablation based on the morphology of malignant cells. *Sci. Rep.* 5, 17157.

20 Ivey, J.W., Latouche, E.L., Richards, M.L., Lesser, G.J., Debinski, W., Davalos, R.V., and Verbridge, S.S.
21 (2017). Enhancing Irreversible Electroporation by Manipulating Cellular Biophysics with a Molecular
22 Adjuvant. *Biophys. J.* 113, 472–480.

23 Jourabchi, N., Beroukhim, K., Tafti, B.A., Kee, S.T., and Lee, E.W. (2014). Irreversible electroporation
24 (NanoKnife) in cancer treatment. *Gastrointest. Interv.* 3, 8–18.

25 Konishi, H., Kikuchi, S., Ochiai, T., Ikoma, H., Kubota, T., Ichikawa, D., Fujiwara, H., Okamoto, K.,
26 Sakakura, C., and Sonoyama, T. (2009). Latrunculin a has a strong anticancer effect in a peritoneal
27 dissemination model of human gastric cancer in mice. *Anticancer Res.* 29, 2091–2097.

28 Kunte, C., Letulé, V., Gehl, J., Dahlstroem, K., Curatolo, P., Rotunno, R., Muir, T., Occhini, A., Bertino, G.,
29 and Powell, B. (2017). Electrochemotherapy in the treatment of metastatic malignant melanoma: a
30 prospective cohort study by InspECT. *Br. J. Dermatol.*

31 Maček-Lebar, A., and Miklavčič, D. (2001). Cell electroporabilization to small molecules in vitro:
32 control by pulse parameters. *Radiol. Oncol.* Vol 35 No 3 2001.

33 Magnus, G., and Keizer, J. (1997). Minimal model of beta-cell mitochondrial Ca²⁺ handling. *Am. J.*
34 *Physiol.* 273, C717-733.

1 Martin, S.S., and Leder, P. (2001). Human MCF10A mammary epithelial cells undergo apoptosis
2 following actin depolymerization that is independent of attachment and rescued by Bcl-2. *Mol. Cell. Biol.*
3 21, 6529–6536.

4 Martin, R.C.G., Agle, S., Schlegel, M., Hayat, T., Scoggins, C.R., McMasters, K.M., and Philips, P. (2017).
5 Efficacy of preoperative immunonutrition in locally advanced pancreatic cancer undergoing irreversible
6 electroporation (IRE). *Eur. J. Surg. Oncol. EJSO* 43, 772–779.

7 Martin II, R.C.G., McFarland, K., Ellis, S., and Velanovich, V. (2012). Irreversible Electroporation Therapy
8 in the Management of Locally Advanced Pancreatic Adenocarcinoma. *J. Am. Coll. Surg.* 215, 361–369.

9 Mashima, T., Naito, M., Noguchi, K., Miller, D.K., Nicholson, D.W., and Tsuruo, T. (1997). Actin cleavage
10 by CPP-32/apopain during the development of apoptosis. *Oncogene* 14, 1007.

11 Mashima, T., Naito, M., and Tsuruo, T. (1999). Caspase-mediated cleavage of cytoskeletal actin plays a
12 positive role in the process of morphological apoptosis. *Oncogene* 18, 2423.

13 Mi, Y., Yao, C., Li, C., Sun, C., Tang, L., and Liu, H. (2009). Apoptosis induction effects of steep pulsed
14 electric fields (SPEF) on human liver cancer cell SMMC-7721 in vitro. *IEEE Trans. Dielectr. Electr. Insul.*
15 16.

16 Morton, W.M., Ayscough, K.R., and McLaughlin, P.J. (2000). Latrunculin alters the actin-monomer
17 subunit interface to prevent polymerization. *Nat. Cell Biol.* 2, 376+.

18 Napotnik, T.B., Wu, Y.-H., Gundersen, M.A., Miklavčič, D., and Vernier, P.T. (2012). Nanosecond electric
19 pulses cause mitochondrial membrane permeabilization in Jurkat cells. *Bioelectromagnetics* 33, 257–
20 264.

21 Napotnik, T.B., Reberšek, M., Vernier, P.T., Mali, B., and Miklavčič, D. (2016). Effects of high voltage
22 nanosecond electric pulses on eukaryotic cells (in vitro): a systematic review. *Bioelectrochemistry* 110,
23 1–12.

24 Neri, S., Mariani, E., Meneghetti, A., Cattini, L., and Facchini, A. (2001). Calcein-acetyoxymethyl
25 cytotoxicity assay: standardization of a method allowing additional analyses on recovered effector cells
26 and supernatants. *Clin. Diagn. Lab. Immunol.* 8, 1131–1135.

27 Pakhomov, A.G., Xiao, S., Pakhomova, O.N., Semenov, I., Kuipers, M.A., and Ibey, B.L. (2014).
28 Disassembly of actin structures by nanosecond pulsed electric field is a downstream effect of cell
29 swelling. *Bio-Electroporation Organised COST TD1104* 100, 88–95.

30 Parlato, S., Giannì Marioli, A.M., Logozzi, M., Lozupone, F., Matarrese, P., Luciani, F., Falchi, M., Malorni,
31 W., and Fais, S. (2000). CD95 (APO-1/Fas) linkage to the actin cytoskeleton through ezrin in human T
32 lymphocytes: a novel regulatory mechanism of the CD95 apoptotic pathway. *EMBO J.* 19, 5123.

33 Pauly, H., Packer, L., and Schwan, H.P. (1960). Electrical properties of mitochondrial membranes. *J. Cell
34 Biol.* 7, 589–601.

1 Plaschke, C.C., Bertino, G., McCaul, J.A., Grau, J.J., de Bree, R., Sersa, G., Occhini, A., Groselj, A., Langdon, C., and Heuveling, D.A. (2017). European Research on Electrochemotherapy in Head and Neck Cancer (EURECA) project: Results from the treatment of mucosal cancers. *Eur. J. Cancer* **87**, 172–181.

4 Puthalakath, H., Villunger, A., O'Reilly, L.A., Beaumont, J.G., Coultas, L., Cheney, R.E., Huang, D.C., and 5 Strasser, A. (2001). Bmf: a proapoptotic BH3-only protein regulated by interaction with the myosin V 6 actin motor complex, activated by anoikis. *Science* **293**, 1829–1832.

7 Reynaud, J.A., Labbe, H., Lequoc, K., Lequoc, D., and Nicolau, C. (1989). Electric field-induced fusion of 8 mitochondria. *FEBS Lett.* **247**, 106–112.

9 Scheffer, H.J., Vroomen, L.G., Nielsen, K., van Tilborg, A.A., Comans, E.F., van Kuijk, C., van der Meijls, 10 B.B., van den Bergh, J., van den Tol, P.M., and Meijerink, M.R. (2015). Colorectal liver metastatic disease: 11 efficacy of irreversible electroporation—a single-arm phase II clinical trial (COLDFIRE-2 trial). *BMC 12 Cancer* **15**, 772.

13 Scheffer, H.J., Vroomen, L.G., de Jong, M.C., Melenhorst, M.C., Zonderhuis, B.M., Daams, F., Vogel, J.A., 14 Besselink, M.G., van Kuijk, C., and Witvliet, J. (2016). Ablation of Locally Advanced Pancreatic Cancer 15 with Percutaneous Irreversible Electroporation: Results of the Phase I/II PANFIRE Study. *Radiology* **282**, 16 585–597.

17 Scheltema, M.J., Van Den Bos, W., de Bruin, D.M., Wijkstra, H., Laguna, M.P., de Reijke, T.M., and de la 18 Rosette, J.J. (2016). Focal vs extended ablation in localized prostate cancer with irreversible 19 electroporation; a multi-center randomized controlled trial. *BMC Cancer* **16**, 299.

20 Schoenbach, K.H., Abou-Ghazala, A., Vithoulkas, T., Alden, R., Turner, R., and Beebe, S. (1997). The effect 21 of pulsed electrical fields on biological cells.

22 Schoenbach, K.H., Hargrave, B., Joshi, R.P., Kolb, J.F., Nuccitelli, R., Osgood, C., Pakhomov, A., Stacey, M., 23 Swanson, R.J., and White, J.A. (2007). Bioelectric effects of intense nanosecond pulses. *Dielectr. Electr. 24 Insul. IEEE Trans. On* **14**, 1088–1109.

25 Schönleitner, P., Schotten, U., and Antoons, G. (2017). Mechanosensitivity of microdomain calcium 26 signalling in the heart. *Prog. Biophys. Mol. Biol.*

27 Schwan, H.P. (1959). Alternating current spectroscopy of biological substances. *Proc. IRE* **47**, 1841–1855.

28 Slee, E.A., Keogh, S.A., and Martin, S.J. (2000). Cleavage of BID during cytotoxic drug and UV radiation- 29 induced apoptosis occurs downstream of the point of Bcl-2 action and is catalysed by caspase-3: a 30 potential feedback loop for amplification of apoptosis-associated mitochondrial cytochrome c release. 31 *Cell Death Differ.* **7**, 556.

32 Stacey, M., Stickley, J., Fox, P., Statler, V., Schoenbach, K., Beebe, S.J., and Buescher, S. (2003). 33 Differential effects in cells exposed to ultra-short, high intensity electric fields: cell survival, DNA 34 damage, and cell cycle analysis. *Mutat. Res. Toxicol. Environ. Mutagen.* **542**, 65–75.

35 Stacey, M., Fox, P., Buescher, S., and Kolb, J. (2011). Nanosecond pulsed electric field induced 36 cytoskeleton, nuclear membrane and telomere damage adversely impact cell survival. 37 *Bioelectrochemistry* **82**, 131–134.

1 Teissie, J. (1986). Adenosine 5'-triphosphate synthesis in *Escherichia coli* submitted to a microsecond
2 electric pulse. *Biochemistry (Mosc.)* 25, 368–373.

3 Thomas, S.G., Huang, S., Li, S., Staiger, C.J., and Franklin-Tong, V.E. (2006). Actin depolymerization is
4 sufficient to induce programmed cell death in self-incompatible pollen. *J. Cell Biol.* 174, 221–229.

5 Thompson Gary L., Roth Caleb, Tolstykh Gleb, Kuipers Marjorie, and Ibey Bennett L. (2014). Disruption of
6 the actin cortex contributes to susceptibility of mammalian cells to nanosecond pulsed electric fields.
7 *Bioelectromagnetics* 35, 262–272.

8 Thomson, K.R., Cheung, W., Ellis, S.J., Federman, D., Kavoudias, H., Loader-Oliver, D., Roberts, S., Evans,
9 P., Ball, C., and Haydon, A. (2011). Investigation of the safety of irreversible electroporation in humans. *J.*
10 *Vasc. Interv. Radiol.* 22, 611–621.

11 Tissera, H., Kodiha, M., and Stochaj, U. (2010). Nuclear envelopes show cell-type specific sensitivity for
12 the permeabilization with digitonin.

13 Trimmer, C.K., Khosla, A., Morgan, M., Stephenson, S.L., Ozayar, A., and Cadeddu, J.A. (2015). Minimally
14 invasive percutaneous treatment of small renal tumors with irreversible electroporation: a single-center
15 experience. *J. Vasc. Interv. Radiol.* 26, 1465–1471.

16 Vercesi, A.E., Bernardes, C.F., Hoffmann, M.E., Gadelha, F.R., and Docampo, R. (1991). Digitonin
17 permeabilization does not affect mitochondrial function and allows the determination of the
18 mitochondrial membrane potential of *Trypanosoma cruzi* in situ. *J. Biol. Chem.* 266, 14431–14434.

19 Wang, Y., Zhu, Y., Ling, Y., Zhang, H., Liu, P., Baluška, F., Šamaj, J., Lin, J., and Wang, Q. (2010). Disruption
20 of actin filaments induces mitochondrial Ca²⁺ release to the cytoplasm and [Ca²⁺]_c changes in
21 *Arabidopsis* root hairs. *BMC Plant Biol.* 10, 53.

22 Wasson, E.M., Ivey, J.W., Verbridge, S.S., and Davalos, R.V. (2017). The Feasibility of Enhancing
23 Susceptibility of Glioblastoma Cells to IRE Using a Calcium Adjuvant. *Ann. Biomed. Eng.* 45, 2535–2547.

24 Xiao, D., Tang, L., Zeng, C., Wang, J., Luo, X., Yao, C., and Sun, C. (2011). Effect of actin cytoskeleton
25 disruption on electric pulse-induced apoptosis and electroporation in tumour cells. *Cell Biol. Int.* 35, 99–
26 104.

27 Zhang, X., Fryknäs, M., Hernlund, E., Fayad, W., De Milito, A., Olofsson, M.H., Gogvadze, V., Dang, L.,
28 Pahlman, S., Schughart, L.A.K., et al. (2014). Induction of mitochondrial dysfunction as a strategy for
29 targeting tumour cells in metabolically compromised microenvironments. *Nat. Commun.* 5, 3295.

30

31

32

33

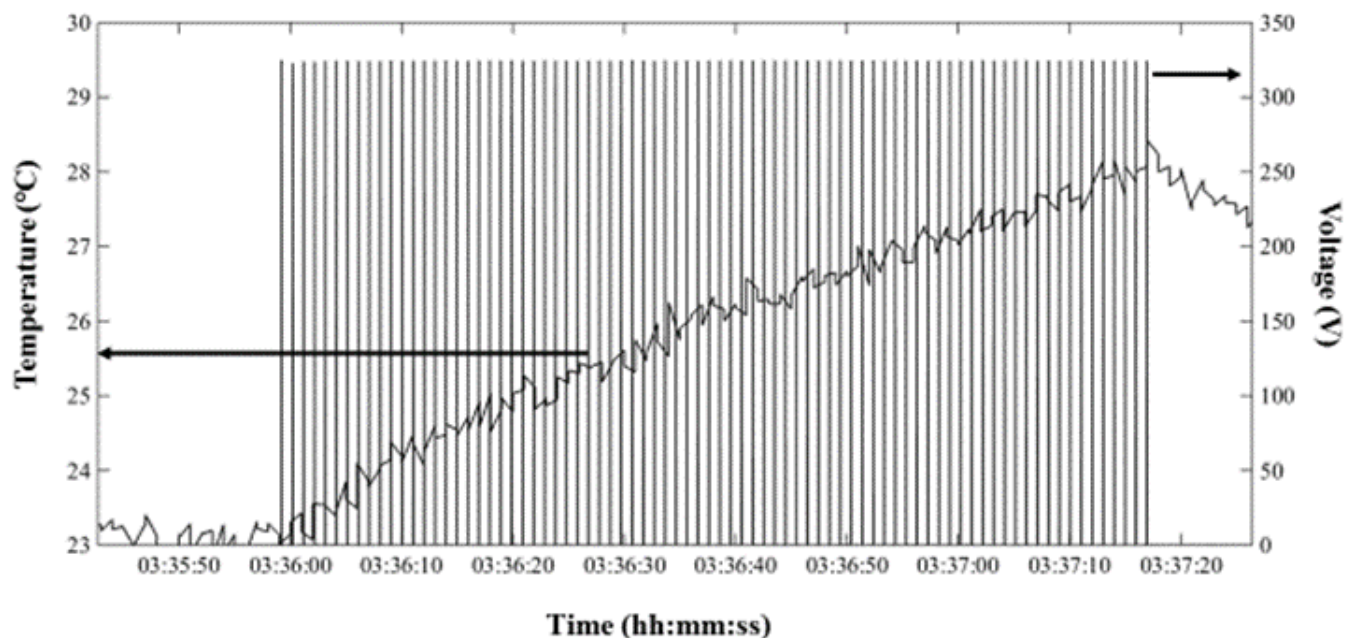
34

35

1

2 **SUPPLEMENTARY FIGURES:**

3



4

5 **Figure S1:** A representative real-time signal captured during treatment showing the profiles of
6 voltage and temperature during pulsed electric field exposure. The voltage signal comprised of 80
7 pulses (represented by the thin lines) each 100 micro-second wide, and a frequency of 1 Hertz.

8

9

10

11

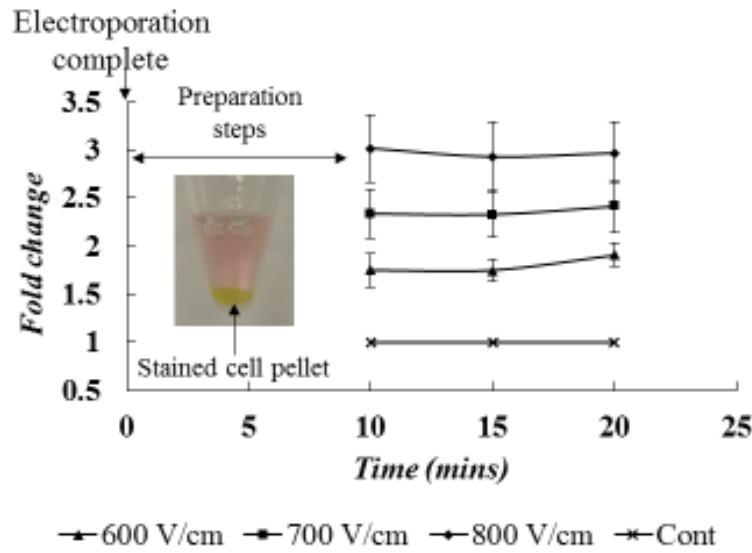
12

13

14

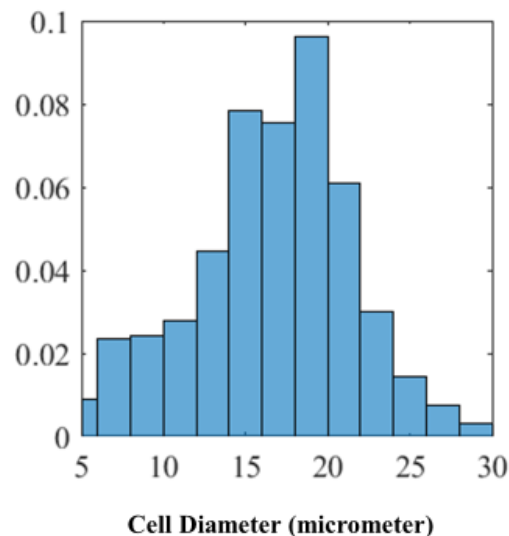
15

16

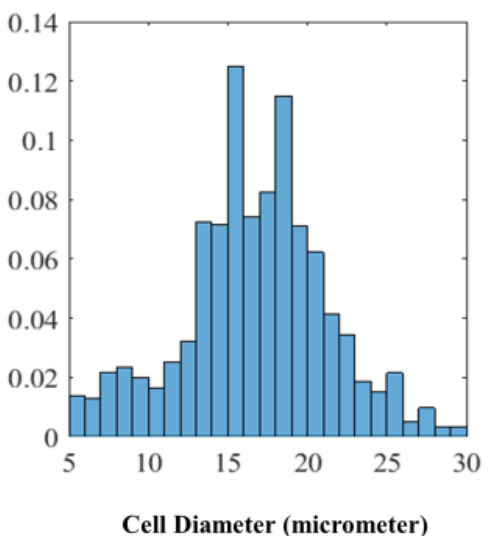


1
2 **Figure S2:** The quantification of cell permeability using Calcein AM assay is shown for cells
3 exposed to PEFs with different field amplitudes.
4
5
6
7
8
9
10
11
12
13
14
15
16
17
18

1
A



B



1

2 **Figure S3:** Probability density function of cell diameter in untreated cells (A) and cells treated
3 with Latrunculin B (B) upon harvesting. The mean size of the cells in suspension between the two
4 groups remained comparably similar.

5